DIFFERENT FORMULATIONS FOR POWER MULTI-WINDING AUTOTRANSFORMER IMPEDANCE VOLTAGE EVALUATION

Alin DOLAN*, Grigore A. CIVIDJIAN*, Ivan YATCHEV**, Gheorghe CALIN*** and Dorin POPA***

*University of Craiova, Electrical Engineering Faculty, Department of Electrical Apparatus and Technologies, 107, bd. Decebal, 200440, Craiova, Romania
E-mail: adolan@elth.ucv.ro, gcividjian@elth.ucv.ro

** Technical University of Sofia, Department of Electrical Apparatus, 1156 Sofia, Bulgaria, E-mail: yatchev@tu-sofia.bg

***ICMET Craiova, 144, Calea Bucuresti, 200515, Craiova, Romania,
E-mail: calin@icmet.ro, dpopa@icmet.ro

Abstract. In the paper, different formulations of 3D finite element method – magnetic vector potential (nodal and edge based) and magnetic scalar potential (nodal based) for power multi-winding autotransformer impedance voltage evaluation are presented. Comparison with earlier 2D finite element method solution and experimental values is also made and error estimation is given. The effectiveness of 3D formulations is analysed from viewpoint of CPU time related to the number of nodes and the influence of PC memory management is discussed.

Keywords: Autotransformer, impedance voltage, 2D-3D FEM, edge formulation, nodal formulation.

INTRODUCTION

The leakage phenomena determine several fundamental properties of a transformer in steady-state operation by influencing the variation of the secondary voltage, the conditions of parallel operation, the additional losses in the transformer and in a abrupt short-circuit mode, by determining the value of short-circuit currents and the resulting mechanical and thermal effects. For this reason, the determination as precise as possible of the short-circuit reactance is one of the principal problems of the transformer [1], [2].

The numerical computation using the finite element method often offers satisfactory solutions. In the paper, different formulations in 3D FEM – magnetic vector potential (nodal and edge based) and magnetic scalar potential (nodal based) – to evaluate the impedance voltage of a power multi-winding autotransformer with regulating windings are comparatively presented. Comparison with earlier 2D FEM axisymmetric solution and experimental values is also made and errors estimation is given.

The edge-based formulation has drawn the attention of many researchers [4], [6]-[9]. It is often considered as better than the nodal-based formulation in the cases of presence of media of different properties due to its main advantage: the elimination of the difficulty of a gauged magnetic vector potential with nodal elements in satisfying the interface conditions on iron/air interfaces, by allowing the normal component of the vector potential to be discontinuous on these interfaces [6], [8]. Edge elements can be used for computing electromagnetic fields in both homogeneous and inhomogeneous domains. Nodal elements can be used in homogeneous (sub)domains only [9]. Although the use of edge elements with a vector potential suffers of numerical stability problems, however, the results obtained by this formulation fit best the measurements [6]. Additionally, the edge element formulation is superior to the nodal element one from the standpoints of the computer storage and the CPU time [4], [7]. In this paper we have analysed the effectiveness of the 3D formulations from viewpoint of CPU time related to the nodes number. The influence of PC memory management is also discussed.

THEORETICAL CONSIDERATIONS

The International Electrotechnical Vocabulary [5] defines the impedance voltage of a multi-winding transformer for the principal tapping, related to a certain pair of windings, as the voltage, required to be applied at rated frequency to the line terminals of one of the windings of a pair for a polyphase transformer, or to the terminals of such a winding for a single-phase transformer, to cause a current to flow through these terminals corresponding to the smaller of the rated power values of both windings of the pair, the terminals of the other winding of the pair being short-circuited and the remaining windings being open-circuited. The various values for the different pairs are normally related to the appropriate reference temperature. The impedance voltage at rated current is usually expressed as a percentage of the rated voltage of the winding to which the voltage is applied.

The short-circuit impedance of a pair of windings is defined, in the same vocabulary, as the equivalent star connection impedance, related to one of the windings, for given tapping and expressed in ohms per phase, at rated frequency, measured between the terminals of a winding when the other winding is short-circuited (the value is normally related to the appropriate reference temperature).

Let w_1, w_2, w_3 and w_R be the numbers of turns of the three windings of power autotransformer (Fig. 1, 2). The secondary winding is connected to the median (principal) tapping of the regulating winding, so that the phase secondary voltage will be [1]-[3], [10]:

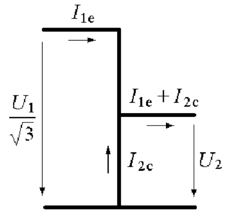

Figure 1. Simplified autotransformer scheme.

(1) $$U_{2ph} = U_{2phr} \cdot \frac{w_2 + \alpha \frac{w_R}{2}}{w_2}, \qquad U_{2phr} = \frac{U_{1r}}{\sqrt{3}} \frac{w_2}{w_1 + w_2},$$ where:

U_{1r} is the primary rating voltage and α is a coefficient depending on the tapping of regulating winding, $-1 \le \alpha \le 1$. To determine the short-circuit parameters for each pair of windings, the energy evaluation approach will be considered.

Primary and secondary winding

The magnetic field energy can be calculated for any arbitrary value of the primary line current I_{1e} (usually close to the primary rated current I_{1r}). For star connection, the phase current will be the same and the corresponding secondary tapping currents result from the equality of the primary and secondary magnetomotive forces:

(2) $$I_{2c} = I_{1eph} \cdot \frac{w_1}{w_2 + \alpha \frac{w_R}{2}}, \qquad I_{1eph} = I_{1e} \approx I_{1r}$$

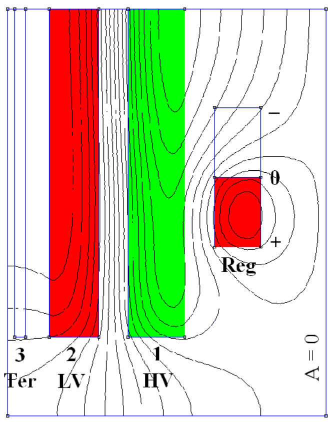

Figure 2. Autotransformer coils disposition with associated flux lines corresponding to “1-2 plus” short circuit test (axisymmetric solution in [10]).

The primary, secondary and regulating winding total cross-sections A_1, A_2 and A_R determine the corresponding current densities:

(3) $$j_1 = w_1 \frac{I_{1eph}}{A_1}; \qquad j_2 = w_2 \frac{I_{2c}}{A_2}; \qquad j_R = \alpha w_R \frac{I_{2c}}{A_R}$$

If W_{12} denotes the magnetic field mean energy per phase, produced by the currents I_{1e} and I_{2c} and evaluated using the finite element method, the referred to primary winding short-circuit reactance will be:

(4) $$x_{k12\%} = 100 \cdot \frac{x_{k12}}{x_{1r}}\ [\%], \qquad x_{k12} = \omega \cdot \frac{2W_{12}}{I_{1e}^2}\ [\Omega], \qquad x_{1r} = \frac{U_{1r}}{\sqrt{3}\, I_{1r}}$$

Primary and tertiary winding

For delta connection of the tertiary winding, the phase currents for energy calculation are:

(5) $$I_{1c} = I_{3eph} \cdot \frac{w_3}{(w_1 + w_2) + \alpha \frac{w_R}{2}}, \qquad I_{3eph} = \frac{I_{3e}}{\sqrt{3}} \approx \frac{I_{3r}}{\sqrt{3}}$$

The corresponding current densities are:

(6) $$j_1 = w_1 \frac{I_{1c}}{A_1}; \qquad j_2 = w_2 \frac{I_{1c}}{A_2}; \qquad j_3 = w_3 \frac{I_{3eph}}{A_3}; \qquad j_R = \alpha w_R \frac{I_{1c}}{A_R}$$

Usually the tertiary winding rated power is smaller, so, according to the International Electrotechnical Vocabulary [5], the short-circuit reactance will be referred to the tertiary winding rated line voltage U_{3r} and line current I_{3r}. If W_{13} is the magnetic field mean energy per phase produced by the currents I_{3e} and I_{1c}, the referred to tertiary winding (equivalent to star connection) short-circuit reactance will be:

(7) $$x_{k13\%} = 100 \cdot \frac{x_{k13}}{x_{3r}}\ [\%], \qquad x_{k13} = \omega \cdot \frac{2W_{13}}{I_{3e}^2}\ [\Omega], \qquad x_{3r} = \frac{U_{3r}}{\sqrt{3}\, I_{3r}}$$

Secondary and tertiary winding

The determination of the short-circuit reactance for the secondary and tertiary windings is similar with the previous case. The secondary and regulating winding currents and the current densities will be:

(8) $$I_{2c} = I_{3eph} \cdot \frac{w_3}{w_2 + \alpha \frac{w_R}{2}}, \qquad I_{3eph} = \frac{I_{3e}}{\sqrt{3}} \approx \frac{I_{3r}}{\sqrt{3}}$$

(9) $$j_2 = w_2 \frac{I_{2c}}{A_2}; \qquad j_3 = w_3 \frac{I_{3eph}}{A_3}; \qquad j_R = \alpha w_R \frac{I_{2c}}{A_R}$$

If W_{23} is the magnetic field mean energy per phase, produced by the currents I_{3e} and I_{2c} and evaluated using the finite element method, the referred to tertiary winding (equivalent to star connection) short-circuit reactance will be:

$$x_{k23\%} = 100 \cdot \frac{x_{k23}}{x_{3r}} \ [\%], \qquad x_{k23} = \omega \cdot \frac{2W_{23}}{I_{3e}^2} \ [\Omega], \qquad x_{3r} = \frac{U_{3r}}{\sqrt{3}\, I_{3r}} \tag{10}$$

MAGNETIC FIELD ENERGY EVALUATION

Due to the relatively small size of the coil conductors, the skin effect in the conductors and in the screens is neglected. Consequently, the coil conductivity is taken equal to zero and the frequency is also considered zero [10].

For analysis of the 3D static magnetic field of the 400/400/80 MVA power autotransformer for 400/231/22 kV, three formulations have been employed – MVP nodal and edge based and MSP nodal based. The MVP-nodal formulation has three degrees of freedom per node: A_x, A_y, and A_z, the magnetic vector potentials in the X, Y and Z directions. The current sources (current conducting regions) are considered as an integral part of the finite element model. The MSP formulation allows to simplify the model, introducing the current sources as that, these do not need to be part of the finite element mesh. The MVP-edge formulation associates degrees of freedom with element edges rather than element nodes. The degrees of freedom are the integrals of the tangential component of the vector potential *A* along the element edges [13].

The numerical results of the 3-D static analysis have been obtained using ANSYS® program, for each pair of windings of the power autotransformer [12]. For automation of the numerical computation, command files have been created using APDL (ANSYS Parameter Design Language).

The mesh was realized using tetrahedral elements. It was considered the instant when the currents, corresponding of the middle column, pass by zero. This has permitted a better thinness of the mesh of the eighth part of the model, due to the created symmetries and by the possibility to mesh only the first column coils. In the analysed domain, the normal conditions of the flux have been considered for the borders, corresponding to the transformer ferromagnetic tank and for interior planes of symmetry, except the vertical plane of symmetry along the three columns, where the parallel flux conditions have been imposed.

In Table 1, the apparent current densities and the magnetic field mean energies per phase, computed by 3D FEM are given for the principal, plus and minus tappings (α = -1, 0, 1). The values of computed short-circuit reactances are compared with the corresponding experimental values of the impedance voltage and with earlier obtained results [10] using 2D FEM with axisymmetric approach. They are presented in Table 2.

Table 1. Current densities and magnetic energies corresponding to the short-circuit tests.

Pair	Tpp.	j_R [A/mm^2]	j_1 [A/mm^2]	j_2 [A/mm^2]	j_3 [A/mm^2]	W [J]			
						2D	3D		
							MSP-N	MVP-E	MVP-N
1-2	0	0	0.799	-0.921	0	21,766	20,049	21,621	20,412
	+	-0.870	0.799	-0.749	0	15,314	14,666	15,444	14,509
	-	1.392	0.799	-1.198	0	43,948	39,920	42,811	39,888
1-3	0	0	0.159	0.252	-2.045	3,768	3,338	3,678	3,579
	+	0.258	0.141	0.222	-2.045	4,372	3,769	4,211	4,068
	-	-0.337	0.184	0.290	-2.045	3,556	3,245	3,502	3,401
2-3	0	0	0	0.436	-2.045	2,512	2,340	2,560	2,451
	+	0.412	0	0.354	-2.045	3,296	2,905	3,285	3,071
	-	-0.659	0	0.567	-2.045	3,850	3,754	3,793	3,586

Table 2. Short-circuit reactances corresponding to the short-circuit tests.

Pair	Tpp.	x_k [Ω]					x_k [%]			
		Exp	2D	3D			2D	3D		
				MSP-N	MVP-E	MVP-N		MSP-N	MVP-E	MVP-N
1-2	0	40.41	41.03	37.79	40.76	38.48	10.26	9.45	10.19	9.62
	+	29.56	28.87	27.64	29.11	27.35	7.22	6.91	7.28	6.84
	-	82.68	82.84	75.25	80.70	75.19	20.71	18.81	20.17	18.80
1-3	0	0.55	0.54	0.48	0.52	0.51	8.88	7.87	8.67	8.43
	+	0.62	0.62	0.54	0.60	0.58	10.30	8.88	9.92	9.58
	-	0.52	0.51	0.46	0.50	0.48	8.38	7.65	8.25	8.01
2-3	0	0.37	0.36	0.33	0.36	0.35	5.92	5.51	6.03	5.78
	+	0.47	0.47	0.41	0.47	0.44	7.77	6.84	7.74	7.24
	-	0.51	0.55	0.54	0.54	0.51	9.07	8.85	8.94	8.45

In table 3 the percentage errors of the numerical solutions related to measurements are presented. The results of 3D computations correspond to the maximum PC capability. The edge formulation is superior to the nodal formulation from the viewpoints of the accuracy. Thus, the MVP-edge based agrees with experiments with an average error of about 2 %, comparably to the earlier 2D FEM computation with 1 %, followed by MVP-nodal based with 7 % and MSP-nodal based with an average error of about 10 %. An exception has been met in “2-3 minus” short-circuit tests case, with bigger errors, probably due to the simplified geometry. Larger memory level can increase the accuracy of nodal formulations.

Table 3. Errors estimation corresponding to the short-circuit tests.

Pair	Tpp.	Errors [%]			
		2D	3D		
			MSP-N	MVP-E	MVP-N
1-2	0	-1.53	6.48	-0.85	4.79
	+	2.35	6.48	1.52	7.48
	-	-0.19	8.99	2.40	9.06
1-3	0	1.62	12.84	3.96	6.55
	+	-0.85	13.07	2.86	6.17
	-	2.89	11.38	4.36	7.12
2-3	0	2.69	9.35	0.82	5.06
	+	0.46	12.26	0.80	7.24
	-	-8.46	-5.76	-6.85	-1.01
Av. Err.		0.93	10.11	1.98	6.68

The computations were run on a PC with 1.5 GB RAM and 1.83 GHz frequency processor. The memory management has direct implications on the working time. When the model requires, additional memory is used from system virtual memory (PC hard disk) to supplement physical memory. This affects strongly the speed performances of the solver, so, only a minimum necessary amount of additionally memory must be allocated [13]. For minimize the working time, different amounts of additional memory have been used during the three analyse phases – pre-processor, processor and post-processor.

A comparison between analysed formulations was made from the viewpoint of the number of nodes, elements, equations and total CPU working time (t_{CPU}). First, the same elements number has been created, for all formulations – the maximum level for witch no additional memory is used, but only real memory. Then, the maximum PC capability has been used to obtain the best thinness of mesh for each formulation. In this case, different amounts of additionally memory have been used and much bigger values of working time have been reached. In order to estimate the working time when no additional memory should be used, for the best thinness mesh cases, we tried to determine the dependency between the elements (or nodes) number and this time (virtual CPU time). Analysing 23 values for each formulation, we have found a relationship:

(11) $$t_{CPU\_virt} = a \cdot n^{c} + b \quad [sec]$$ where

n is the nodes number and a, b, c have been determined by least squares method (tab. 4). The dependency CPU time – number of nodes is printed in Figure 3.

Table 4. Coefficients in virtual CPU time estimation

	MSP-N	MVP-E	MVP-N
a	$0.95 \cdot 10^{-3}$	$4.27 \cdot 10^{-6}$	$0.13 \cdot 10^{-3}$
b	41.02	66.92	45.54
c	1.20	1.47	1.39

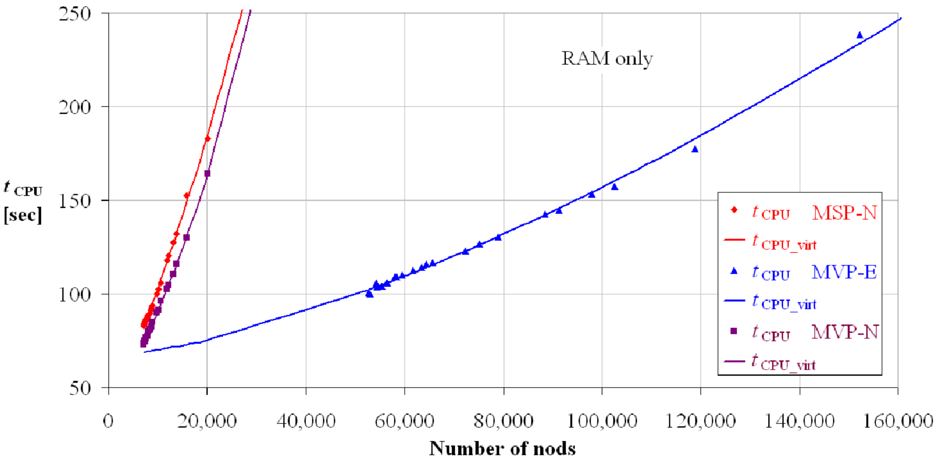

Figure 3. CPU time versus number of nodes.

We could compare the virtual CPU time with the real time obtained using supplementary memory. The results presented in table 5 show that using additional memory in range of 1.5-3 GB, the working time can increase up to 10–24 times.

In all cases, the edge formulation is better than nodal formulation from the viewpoint of the CPU working time related to the nods number.

Table 5. CPU time for "1-2 plus" short-circuit test.

Real memory 1.5 GB	No additional memory			Maximum PC capability		
	MSP-N	MVP-E	MVP-N	MSP-N	MVP-E	MVP-N
Nodes	20,089	152,316	20,089	124,424	573,349	170,913
Elements	109,294	109,294	109,294	723,016	421,501	999,954
Equations	18,813	109,383	56,046	121,060	412,800	501,398
Add. mem.	0 GB	0 GB	0 GB	1.5-2 GB	1.5-2 GB	2-3 GB
t_{CPU} [sec]	183	238	164	29,487	11,586	55,583
t_{CPU_virt} [sec] – for no RAM limit				1,333	1,231	2,345
t_{CPU} increasing rate				22 x	10 x	24 x

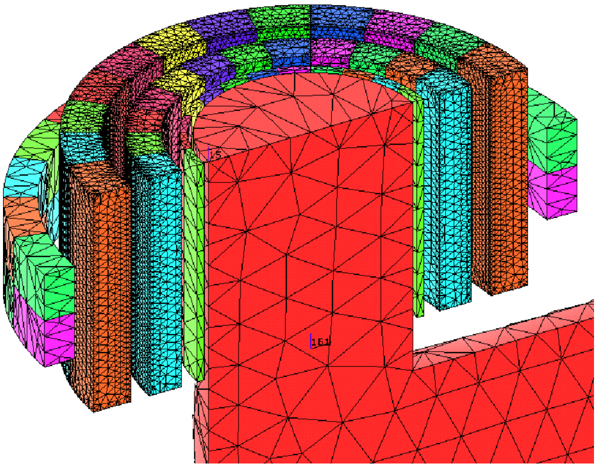

Figure 4. Mesh model perspective.

Using the visualization facilities offered by ANSYS® program, the figure 4 shows the 3D symmetry-plane perspective of the model with associated mesh. The magnetic field distributions on the borders and symmetry planes are shown in figure 5, for primary-secondary windings short-circuit test at plus tapping of the regulating winding, MVP edge formulation – the 3D solution with the best accuracy.

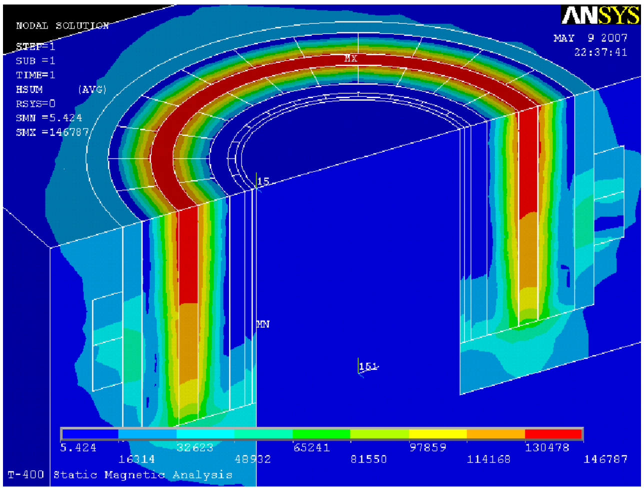

Figure 5. Magnetic field distributions for primary-secondary windings short-circuit test at plus tapping of the regulating winding.

CONCLUSIONS

In the case of regulating windings, the impedance voltage cannot more be accurately determined using classical methods and FEM must be used. At 50 Hz the transformer leakage magnetic flux can be well approximated with the static flux (0 Hz).

The comparison of numerical 3D FEM computed values of the impedance voltage, of the studied 400 MVA autotransformer, with the corresponding experimental data confirms that the edge-based formulation gives more accurate results than the nodal-based formulation. The MVP-edge based agrees with experiments with an average error of about 2 %, comparably to the earlier 2D FEM computation with 1 %, followed by MVP-nodal based with 7 % and MSP-nodal based with an average error of about 10 %. Larger memory can increase the accuracy of nodal formulations. The effectiveness of edge formulation is also proved by the minimum CPU time related to nodes number. Best accuracy can be reached using additional memory (PC hard disc) but this increases strongly the working time. 3D approach requires much more hardware resources than the 2D approach but it is preferable for nonsymmetrical configurations.

REFERENCES

[1] G. N. Petrov. *Electrical machines, part 1 - The transformers* (in Russian). GEI, Moscow, 1956.

[2] M. Kostenko and L. Piotrovski. *Electrical machines, tome 1* (in French). Mir, Moscow 1976.

[3] P. M. Tihomirov. *Calculation of Transformers* (in Russian). Energoatomizdat, Moscow, 1986.

[4] T. Nakata, N. Takahashi, K. Fujiwara, T. Imai and K. Muramatsu. Comparison of various methods of analysis and finite elements in 3-D magnetic field analysis. IEEE Transactions on Magnetics, vol. 27, No. 5, 1991, pp. 4073-4076.

[5] Electricity, Electronics and Telecommunications. *IEC Multilingual Dictionary*, vol.1. Elsevier, Amsterdam, New-York, Tokyo, Oxford, 1992.

[6] K. Preis, I. Bardi, O. Biro, C. Magele, G. Vrisk and K. R. Richter. Different finite element formulations of 3D magnetostatic fields. IEEE Transactions on Magnetics, vol. 28, No. 2, 1992, pp. 1056-1059.

[7] N. Nakata, T. Nakata, K. Fujiwara and T. Imai. Investigation of effectiveness of edge elements. IEEE Transactions on Magnetics, vol. 28, No. 2, 1992, pp. 1619-1622.

[8] J. P. Webb. Edge elements and what they can do for you. IEEE Transactions on Magnetics, vol. 29, No. 2, 1993, pp. 1460-1465.

[9] G. Mur. Edge elements, their advantages and their disadvantages. IEEE Transactions on Magnetics, vol. 30, No. 5, 1994, pp. 3552-3557.

[10] G. A. Cividjian, G. Calin, D. Popa and A. Dolan. Impedance voltage of power multi-winding autotransformer. XIV-th International Symposium on Electrical Apparatus and Technologies, SIELA-2005. Plovdiv, Bulgaria, vol. I, 2005, pp. 39-44.

[11] A. Dolan, I. Yatchev and K. Hinov. Comparison of different formulations and techniques for 3D static force computation of a T-shaped electromagnet, International PhD Seminar - Computational Electromagnetics and Technical Applications. Banja Luka, Bosnia and Herzegovina, 2006, pp. 73-77.

[12] A. Dolan, G. A. Cividjian, I. Yatchev, G. Calin and D. Popa. Three dimensional numerical solution for impedance voltage of power multi-winding autotransformer. VIII-th International Conference on Applied and Theoretical Electricity, ICATE-2006. Baile Herculane, Romania, 2006, pp. 326-329.

[13] ANSYS Documentation. *ANSYS. Inc. Theory Reference*.